

Space astrometry of the very massive $\sim 150 M_{\odot}$ candidate runaway star VFTS682

M. Renzo¹, S. E. de Mink¹, D. J. Lennon², I. Platais³, R. P. van der Marel^{3,4}, E. Laplace¹, J. M. Bestenlehner⁵, C. J. Evans⁶, V. Hénault-Brunet⁷, S. Justham^{8,9,1}, A. de Koter¹, N. Langer¹⁰, F. Najarro¹¹, H. Sana¹², F. R. N. Schneider¹³, J. S. Vink¹⁴

Accepted XXX. Received YYY; in original form ZZZ
Affiliations can be found at the end of this manuscript

ABSTRACT

How very massive stars form is still an open question in astrophysics. VFTS682 is among the most massive stars known, with an inferred initial mass of $\gtrsim 150 M_{\odot}$. It is located in 30 Doradus at a projected distance of 29 pc from the central cluster R136. Its apparent isolation led to two intriguing hypotheses: either it formed in relative isolation or it was ejected dynamically from the cluster. We investigate the kinematics of VFTS682 as obtained by *Gaia* and multi-epoch *Hubble Space Telescope* astrometry. We derive a projected velocity relative to the cluster of $38 \pm 17 \text{ km s}^{-1}$ (1σ confidence interval). Although the error bars are substantial, two independent measures suggest that VFTS682 is a runaway ejected from the central cluster. This hypothesis is further supported by a variety of circumstantial clues. The central cluster is known to harbor other stars more massive than $150 M_{\odot}$ of similar spectral type and recent astrometric studies on VFTS16 (and possibly VFTS72) provide direct evidence that the cluster can eject some of its most massive members, in agreement with theoretical predictions. If future data confirm the runaway nature, this would make VFTS682 the most massive runaway star known to date.

Key words: stars: astrometry, kinematics and dynamics, individual: VFTS682

1 INTRODUCTION

How massive stars form is one of the major longstanding questions in astrophysics (e.g., Zinnecker & Yorke 2007). Obtaining clues from observations is challenging, because massive stars are intrinsically rare, evolve fast, typically reside in dense groups, and remain enshrouded in their parent cloud during the entirety of the formation process. Important progress has been made on the theoretical side, (e.g. Bate 2009; Kuiper et al. 2015; Rosen et al. 2016), but the simulations remain challenging.

It has been proposed that most, if not all, stars form in clusters (Lada & Lada 2003, and references therein). In this picture, field stars are primarily the result of the dissolution of dense groups. However, a significant population of massive stars exists in relative isolation, far from dense clusters or OB associations and their origin remains a matter of debate (Gvaramadze et al. 2012; Lamb et al. 2016; Ward & Kruijssen 2018). One hypothesis to explain the population of relatively isolated massive stars is that they formed in the field (e.g., Parker & Goodwin 2007). Another hypothesis is that these massive stars were ejected from the clusters

in which they formed. Such ejections may result from dynamical interactions (e.g., Poveda et al. 1967) or from the disruption of binary systems at the death of the companion star (e.g., Blaauw 1961; Renzo et al. 2018).

One of the most extreme examples that has been considered in this debate is the very massive star VFTS682 (Bestenlehner et al. 2011; Bressert et al. 2012). This star is located in the field of the 30 Doradus (30Dor) region in the Large Magellanic Cloud (LMC) and was studied as part of the multi-epoch spectroscopic VLT-FLAMES Tarantula Survey (VFTS, Evans et al. 2011). It is a hydrogen-rich Wolf-Rayet star of spectral type WNh5. Spectral analysis and comparison with evolutionary models lead to an inferred present-day mass of $137.8^{+27.5}_{-15.9} M_{\odot}$ corresponding to an initial mass of $150.0^{+28.7}_{-17.4} M_{\odot}$ (Schneider et al. 2018). This makes VFTS682 one of the most massive stars known and one of the most extreme objects in the region. From the spectral point of view, it is reminiscent of the very massive stars in the core of the R136 cluster (de Koter et al. 1997; Crowther et al. 2010, 2016). In particular, a remarkable similarity exist between the spectra of VFTS682 and R136a3 (Rubio-Díez et al. 2017).

Table 1. Stellar parameters of VFTS682.

Parameter	Units	Value	Ref.
present day mass	[M_{\odot}]	$137.8^{+27.5}_{-15.9}$	(1)
initial mass	[M_{\odot}]	$150.0^{+28.7}_{-17.4}$	(1)
age	[Myr]	1.0 ± 0.2	(1)
mass loss rate	$\log_{10}(\dot{M}/[M_{\odot} \text{ yr}^{-1}])$	-4.1 ± 0.2	(2)

The quoted uncertainties are statistical, and do not include systematic effects in the modeling. (1) Schneider et al. (2018) (2) Bestenlehner et al. (2011)

VFTS682 stands out by its relative isolation at a projected distance of 119.4 arcseconds, corresponding to 29 pc, from the star cluster R136. Bestenlehner et al. (2011) considered two possible explanations for the offset: either the star formed in situ as an isolated massive star, or it was ejected from R136. N-body simulations indicate that the ejection of very massive stars like VFTS682 is expected (e.g. Fujii & Portegies Zwart 2011; Banerjee et al. 2012). The capability of young clusters of ejecting a large number of (very) massive stars is supported by the recent findings of proper motion studies (e.g., Lennon et al. 2018; Drew et al. 2018).

Platais et al. (2015, 2018) analyzed multi-epoch *Hubble Space Telescope* (HST) photometry and identified 10 stars likely ejected from R136. Lennon et al. (2018) investigated the kinematics of isolated O-type stars in the region using the second *Gaia* data release (DR2, Gaia Collaboration et al. 2016, 2018) and showed that the proper motion, position and direction of the $\sim 100 M_{\odot}$ star VFTS16 is consistent with a runaway origin from R136. They found a less clear case for VFTS72, and in both cases some tension between the kinematic age of these stars and their apparent age remains.

In this paper we present an analysis of the new kinematic constraints for VFTS682 provided by *Gaia* DR2 and constraints from HST proper motions by Platais et al. (2018). We discuss the implications of the hypothesis that VFTS682 is a slow runaway star ejected from R136.

2 OBSERVATIONS

The WNH5 star VFTS682, located at right ascension (RA) $05^{\text{h}}38^{\text{m}}55.510^{\text{s}}$ and declination (DEC) $-69^{\circ}04'26.72''$ (J2000), was observed as part of the multi-epoch, spectroscopic VFTS campaign covering $\lambda 4000\text{--}7000$ (Evans et al. 2011). Bestenlehner et al. (2011) analyzed the spectra to infer the stellar parameters and measure an extinction of $A_V = 4.45 \pm 0.12$, implying a luminosity of $\log_{10}(L/L_{\odot}) = 6.5 \pm 0.2$, making this one of the most luminous stars in the region. The absence of periodic radial velocity (RV) variations suggests that the star is unlikely to have close binary companions (Bestenlehner et al. 2011), unless the orbital inclination is very high. Bayesian fits of the stellar parameters against evolutionary tracks (Brott et al. 2011; Köhler et al. 2015) using the BONNSAI code (Schneider et al. 2014, 2017) provide estimates for the age, present mass and initial mass, as given in Table 1.

VFTS682 is not a bright X-ray point source. It was not detected in the *Chandra* survey of Townsley et al. (2006), and shows a few counts in the deeper survey of Townsley et al. (2014). The X-ray luminosity of VFTS682 is significantly lower than known massive binaries in the region, which suggests the absence of colliding winds. These would

Table 2. Kinematics of VFTS682.

Parameter	Units	Value	Ref.
<i>Absolute and relative position</i>			
R _A _{VFTS682}	[degrees]	84.73136339876477	(1)
D _E _C _{VFTS682}	[degrees]	-69.07411071794998	(1)
R _A _{R136}	[degrees]	84.6750	(2)
D _E _C _{R136}	[degrees]	-69.1006	(2)
δ _{RA}	[mas]	0.0547	(3, 5)
δ _{DEC}	[mas]	0.0268	(3, 5)
d_{\parallel}	[arcsec]	119.4	(3)
L_{\parallel}	[pc]	29	(3)
<i>Gaia absolute proper motion for VFTS682 and the region</i>			
μ_{RA}	[mas yr $^{-1}$]	1.84 ± 0.07	(1)
μ_{DEC}	[mas yr $^{-1}$]	0.79 ± 0.08	(1)
$\rho(\mu_{\text{RA}}, \mu_{\text{DEC}})$		0.0226	(1)
$\langle \mu_{\text{RA}} \rangle_{\text{R136}}$	[mas yr $^{-1}$]	1.74 ± 0.01	(4)
$\langle \mu_{\text{DEC}} \rangle_{\text{R136}}$	[mas yr $^{-1}$]	0.70 ± 0.02	(4)
<i>Gaia relative proper motion for VFTS682</i>			
$\delta\mu_{\text{RA}}$	[mas yr $^{-1}$]	0.10 ± 0.08	(1,6)
$\delta\mu_{\text{DEC}}$	[mas yr $^{-1}$]	0.08 ± 0.10	(1,6)
$\delta\mu_{\text{Gaia}}$	[mas yr $^{-1}$]	0.13 ± 0.09	(1,6)
v_{2D}	[km s $^{-1}$]	32 ± 21	(1,6)
θ_{Gaia}	[degrees]	14^{+36}_{-31}	(1,6)
<i>HST relative proper motion for VFTS682</i>			
$\delta\mu_{\text{RA,HST}}$	[mas yr $^{-1}$]	0.02 ± 0.10	(5)
$\delta\mu_{\text{DEC,HST}}$	[mas yr $^{-1}$]	0.19 ± 0.09	(5)
$\delta\mu_{\text{HST}}$	[mas yr $^{-1}$]	0.19 ± 0.09	(5)
$v_{2D,\text{HST}}$	[km s $^{-1}$]	45 ± 21	(5)
θ_{HST}	[degrees]	-30^{+24}_{-51}	(1,6)
<i>Weighted average relative proper motion for VFTS682</i>			
$\delta\mu_{\text{RA,avg}}$	[mas yr $^{-1}$]	0.08 ± 0.07	(6)
$\delta\mu_{\text{DEC,avg}}$	[mas yr $^{-1}$]	0.14 ± 0.07	(6)
$\delta\mu_{\text{avg}}$	[mas yr $^{-1}$]	0.16 ± 0.07	(6)
$v_{2D,\text{avg}}$	[km s $^{-1}$]	38 ± 17	(6)
<i>Expected proper motion if ejected from R136 at age zero</i>			
v_{2D}	[km s $^{-1}$]	29 ± 6	(3)
θ	[degrees]	~ 0	

The error on the RA and DEC positions, are of order $\sim 10^{-2}$ mas yr $^{-1}$ in *Gaia* DR2. $\rho(\mu_{\text{RA}}, \mu_{\text{DEC}})$ is the correlation coefficient. The position angle θ is defined such that $\theta = 0$ for radial motion away from R136. We neglect the error bars on $\langle \mu_{\text{RA}} \rangle_{\text{R136}}$ and $\langle \mu_{\text{DEC}} \rangle_{\text{R136}}$ to determine the uncertainty on θ_{Gaia} . (1) Gaia Collaboration et al. (2018), (2) Hénault-Brunet et al. (2012), (3) Bestenlehner et al. (2011), (4) Lennon et al. (2018), (5) Platais et al. (2018) and (6) this study.

be expected in the presence of companions even for extreme mass ratios, given the extremely large mass of VFTS682.

This star is also relatively isolated in the (near) infrared. The nearest bright (near-)infrared sources detected by *Spitzer* (Meixner et al. 2006) and resolved in the *VISTA* Magellanic Clouds Survey (Cioni et al. 2011) are located at a distance of about 10 arcsecond, i.e. about 2.4 pc. Walborn et al. (2013) speculate that these nearby young stars may represent a case of star formation triggered by the the wind of VFTS682.

The V-band light curve of VFTS682 shows variations at a $\sim 10\%$ level on a timescale of years, which is unusual

for Wolf-Rayet stars and more typical for Luminous Blue Variable (LBV) stars (Udalski et al. 2008; Bestenlehner et al. 2011). It also shows a mid-infrared excess (Gruendl & Chu 2009).

Estimates of the radial velocity are complicated by the variable, possibly inhomogeneous, optically thick wind typical of emission line stars. Bestenlehner et al. (2011) estimate a mass loss rate of $\log_{10}(\dot{M}/[M_{\odot} \text{ yr}^{-1}]) = -4.1 \pm 0.2$, not accounting for the possible effect of clumping. We therefore caution against over-interpreting the radial velocities estimates. Bestenlehner et al. (2011) estimate a RV of $300 \pm 10 \text{ km s}^{-1}$ using the NV $\lambda 4944$ line, which is offset from the average radial velocity of the region of $270 \pm 10 \text{ km s}^{-1}$. This was suggested as indicating a runaway nature, but it is no proof of it. Bressert et al. (2012) note an offset compared between the RV of the star and the nebular lines from the gas filaments in its vicinity. This is consistent with the expectation if the star was not formed in situ. We will refrain from using the RV measurements in this work, and focus on the velocities on the plane of the sky.

We adopt a distance to the LMC of 50 kpc. The error on the distance determination is small ($\lesssim 2\%$, Pietrzyński et al. 2013) and any possible offset in the radial direction between R136 or VFTS682 and the distance we adopted for the LMC is probably much smaller ($\sim 0.5\%$, e.g., Luks & Rohlfs 1992). These uncertainties are negligible compared to the errors in the proper motion discussed below.

2.1 Gaia astrometry for VFTS682

VFTS682 is identified with the source id 4657685637907503744 in the *Gaia* DR2 catalog as a 15.65 mag star in the G band (Gaia Collaboration et al. 2016, 2018). The number of visibility periods, i.e., groups of observations separated from other groups by a gap of at least four days, used in the astrometric solution is seventeen. The reported astrometric excess noise is zero. These values suggest that the *Gaia* DR2 data for VFTS682 are reliable.

Gaia provides absolute proper motions. To determine the relative proper motion with respect to R136, we follow Lennon et al. (2018) to define the motion of the local frame of reference using the average proper motion of nearby stars with reliable astrometric data. They selected bright ($G < 17$) stars within 0.05 degrees of R136 and exclude sources with proper motion error bars greater than 0.1 mas yr^{-1} in both coordinates (see their Sect. 2.1). Using this definition of the local frame, we compute the relative proper motion $\delta\mu_{RA}$ and $\delta\mu_{DEC}$. We also compute the total projected 2D velocity v_{2D} and the angle θ between the direction of motion and the vector connecting the center of R136 with the current position of VFTS682, i.e. such that $\theta = 0$ is the angle corresponding to perfectly radial motion away from R136. All kinematic quantities are provided in Table 2.

2.2 HST (WFC3/UVIS) astrometry for VFTS682

The 30 Dor region was targeted by a two-epoch photometric campaign with HST providing observations in the F775W filter in October 2011 and October 2014 (GO-12499; P.I.: D. J. Lennon). Platais et al. (2015, 2018) analyzed the HST data to determine the relative proper motions and identify candidate runaway stars. The brightest stars ($V < 14$) are saturated in the data set and have been excluded from the analysis. The high extinction around VFTS682 makes it redder

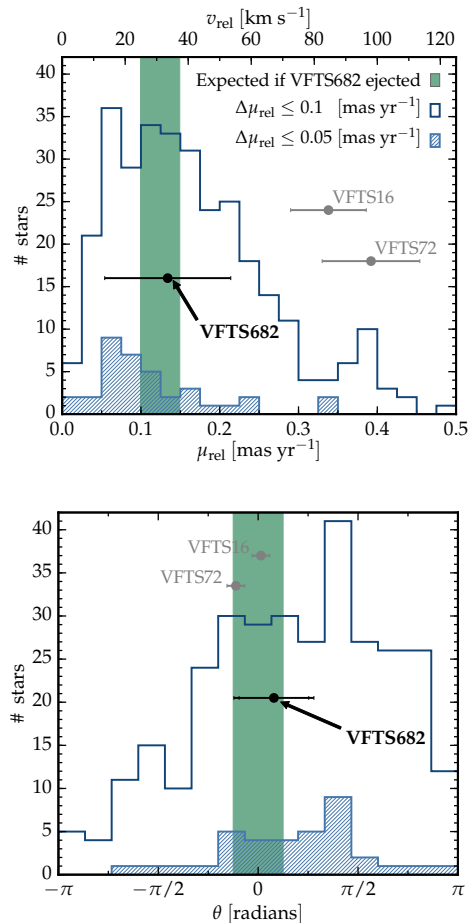


Figure 1. Distribution of OB-type and Wolf-Rayet stars in proper motion relative to R136 (top panel) and proper motion angle (bottom panel), from *Gaia* DR2. Although VFTS682 is not an outlier, its relative proper motion matches the value expected for an early dynamical ejection. In both panels, the green vertical bands highlight these expectations, the dark blue histograms contain 317 stars with error bars smaller than $0.1 \text{ mas yr}^{-1} \approx 25 \text{ km s}^{-1}$ at 50 kpc, the lighter blue histograms contain 36 stars with error bars smaller than 0.05 mas yr^{-1} . The peak at $\theta \approx \pi/2$ in the bottom panel is due to stars belonging to NGC2060.

and fainter ($V = 16.08$, $B - V = 0.58$, Evans et al. 2011), hence it has reasonably accurate HST astrometry with the WFC3/UVIS camera. This star did not pass a full set of stringent conditions to be considered as a candidate runaway (Platais et al. 2018). In retrospect, VFTS682 may have been included in the list of likely OB runaway stars, and it is identified with the ID source 330375 in their catalog. Therefore, their measurements provide useful complementary estimate of the proper motion of VFTS682 independent from the *Gaia* data.

The HST study provides proper motions that are relative to the bulk motion of the majority of the stars in the field of view. The full 30 Dor field is covered by different pointings and there is some systematic distortion. However, even for stars far from 30 Dor the effect is small, no more than 0.05 mas yr^{-1} across the whole 30 Dor field. The effect is much smaller for stars close to the center of field, such as VFTS 682 (Platais et al. 2018). We can therefore use the relative proper motion (Table 2) as a good estimate for the proper motion relative to R136.

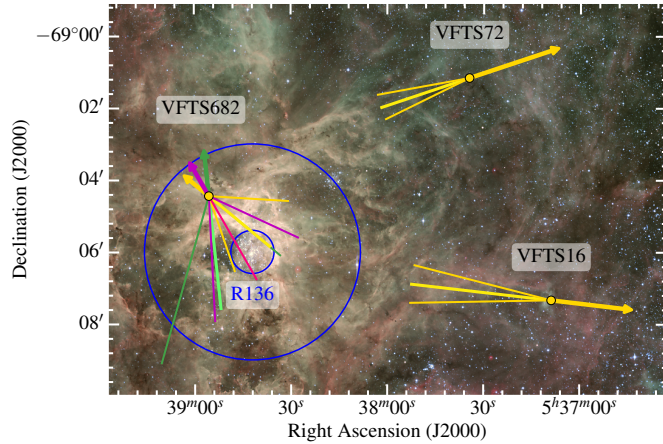


Figure 2. The thick purple arrow shows proper motion relative to R136 for VFTS682 averaging the *Gaia* DR2 and HST astrometry, multiplied by 0.4 Myr. The extension in the opposite direction is proportional to the apparent age of the star, and the thin lines illustrate the error cone on the potential origin. The yellow arrows show the *Gaia* DR2 results alone, and the green arrow the HST results alone. The two blue circles indicate the regions of radii 0.01 and 0.05 degrees around the core of R136.

3 THE KINEMATICS OF VFTS682

The black points in Fig. 1 show the proper motion (left panel) and the projected flight direction (right panel) relative to R136 of VFTS682 from *Gaia* DR2. θ is the angle between the projected radial direction from the center of R136 to each star and its projected relative proper motion (see also Fig. 2). Dynamical ejections from the cluster should produce close to radial ejections, i.e. $\theta \approx 0$. The green vertical bands highlight the expectations for these two quantities if VFTS682 were ejected from R136 early in its lifetime. For comparison, we also show the relative proper motion of VFTS16 and VFTS72 (gray points), and the distribution in relative proper motion and flight direction for all the VFTS OB-type and Wolf-Rayet stars with *Gaia* DR2 errors on the proper motion components of less than 0.1 mas yr^{-1} (dark blue lines, including VFTS682), and less than 0.05 mas yr^{-1} (light hatched blue). Although the error bars are substantial and VFTS682 is not an outlier compared to other OB-type and Wolf-Rayet stars, the agreement suggests that the star is indeed a “slow runaway” as suggested by Bestenlehner et al. (2011).

Subtracting the mean motion of R136, we obtain relative proper motions (projected velocities) of $\delta\mu_{\text{Gaia}} = 0.13 \pm 0.09 \text{ mas yr}^{-1} (32 \pm 21 \text{ km s}^{-1})$ and $\delta\mu_{\text{HST}} = 0.19 \pm 0.09 \text{ mas yr}^{-1} (45 \pm 21 \text{ km s}^{-1})$. Both values are consistent with each other, but also with no motion relative to R136 within 2σ . The average (weighted with $1/\sigma^2$) of these two independent measurements is $\delta\mu_{\text{avg}} = 0.16 \pm 0.07 \text{ mas yr}^{-1} (38 \pm 17 \text{ km s}^{-1})$.

Figure 2 shows the projected motion of VFTS682 relative to R136 on the sky. We also show VFTS16 and VFTS72 (see Lennon et al. 2018). The thick yellow arrows are proportional to the relative proper motion from *Gaia* DR2, and the thick green line illustrates the relative proper motion from HST. The error cone on the direction of motion is il-

lustrated by the corresponding extension in the direction opposite to the motion, and we also show the most likely origin of the stars accounting for their apparent age. This figure illustrates that R136 is the most likely origin of these stars, although the large error bars prevent a robust identification for VFTS682, and there is some tension between the apparent age and the present day distance from the cluster core for VFTS16 and VFTS72 (Lennon et al. 2018). We note that VFTS72 has a small radial velocity, while VFTS16 (and possibly VFTS682) has large peculiar radial velocity and therefore accurate distances along the line of sight are needed to constrain the flight direction in three dimensions.

Assuming VFTS682 indeed originates from R136, we can calculate its kinematic age as:

$$\tau_{\text{kin}} = \frac{d_{\parallel}}{\delta\mu_{\text{avg}}} \simeq \frac{119.4 \text{ arcsec}}{0.16 \text{ mas yr}^{-1}} \simeq 0.7 \pm 0.3 \text{ Myr}, \quad (1)$$

where $d_{\parallel} = 119.4 \text{ arcsec}$ is the angular distance from VFTS682 to the core of the cluster (Bestenlehner et al. 2011). The kinematic age τ_{kin} is consistent with an early ejection from the cluster (see Table 1).

In summary, both *Gaia* and HST relative proper motions are consistent with the dynamical ejection of VFTS682 from the cluster, although we cannot confidently rule out the counter hypothesis.

4 DISCUSSION

Based on our results, we consider likely that VFTS682 is the most massive runaway known to date, with a two-dimensional projected velocity with respect to R136 of $38 \pm 17 \text{ km s}^{-1}$ (averaging the *Gaia* DR2 and HST results). Due to the large error bars, this result will need to be revisited with future astrometric data.

If confirmed, it means that isolated star formation is *not* required to explain the isolation of VFTS682. Its proper motion suggests that it was ejected from the cluster R136 0.7 ± 0.3 Myr ago, which is compatible with the evolutionary age of the star. If the cluster age ($\lesssim 2$ Myr, Crowther et al. 2010; Sabbi et al. 2012) is indeed smaller than the shortest stellar lifetime (~ 3 Myr, Brott et al. 2011; Köhler et al. 2015; Zapartas et al. 2017), the ejection of VFTS682 from the disruption of a binary by a supernova is excluded. The kinematic age we infer is smaller than the kinematic age of ~ 1.5 Myr for VFTS16 found in Lennon et al. (2018), which indicates that VFTS682 was ejected later than VFTS16, and potentially later than VFTS72 too.

If the star were ejected dynamically, its isolation makes it an ideal target to constrain the stellar physics of stars with masses well above $\sim 100 M_{\odot}$ in the inner cluster, while avoiding crowding issues. Moreover, its exceptionally large mass raises the question of which stars must populate the core of the cluster. N-body dynamics typically ejects the least massive star among those interacting (e.g., Banerjee et al. 2012). Just based on the kinematic properties of VFTS682, we would expect several stars with initial masses larger than $\sim 150 M_{\odot}$ in the cluster R136, as it is observed.

The N-body simulations of Banerjee et al. (2012) suggest that VFTS682 was ejected from R136. In their model, they relied on (dynamically driven) stellar mergers to explain the high masses of VFTS682 and the massive members of R136. They demonstrated that the cluster potential does not significantly change the velocity of the star after

the ejection. To eject such a massive object, the cluster is expected to have produced a large number of massive runaways. Indeed, several isolated massive stars are observed in the region (Evans et al. 2010; Lennon et al. 2018), some with known large radial velocities and/or proper motion. A comprehensive study of the kinematic properties of all the massive stars surrounding R136 could shed light on whether some can be unequivocally identified as merger products, but also on the initial conditions for the cluster dynamics (e.g., Oh & Kroupa 2016), and whether it formed via a monolithic collapse, or as a (potentially ongoing) merger of several substructures (e.g., Sabbi et al. 2012).

Also Fujii & Portegies Zwart (2011) suggest that early in the evolution of a cluster, dynamical interactions form an extremely massive binary, which then tightens its orbit by ejecting other stars. The spectral similarities between VFTS682 and stars in the core of R136 are in agreement with this ‘bully binary’ model. Interpreting the kinematics of VFTS682 through the lens of their simulations suggests the presence of a close binary with total mass $M_1 + M_2 \gtrsim 300 M_{\odot}$ in the core of the cluster. The kinematic age of VFTS682 puts an upper limit to the timescale to form the ‘bully binary’ in R136. If identified, such a binary might be an ideal observational candidate for a dynamically formed progenitor system of a binary black-hole, provided that stars this massive can avoid a pair-instability supernova (e.g., Rakavy & Shaviv 1967) at LMC metallicity (see also Langer et al. 2007). Similarly, the final fate of VFTS682 could be either a pair-instability supernova without compact remnant formation, or possibly direct collapse to a black hole above the pair-instability mass gap. The amount of mass loss of these stars will determine their final core mass and thus their final fate.

VFTS682 is potentially the most massive runaway known to date, and its ejection from the cluster R136 likely implies that it is only the ‘tip of the iceberg’ of possibly extremely massive runaways in the region. Studies of this population, enabled by recent and future HST and *Gaia* observations will put constraints on the evolution of these extreme stars, together with the formation and evolution of the central cluster itself.

REFERENCES

- Banerjee S., Kroupa P., Oh S., 2012, *ApJ*, **746**, 15
 Bate M. R., 2009, *MNRAS*, **392**, 590
 Bestenlehner J. M., et al., 2011, *A&A*, **530**, L14
 Blaauw A., 1961, *Bull. Astron. Inst. Netherlands*, **15**, 265
 Bressert E., et al., 2012, *A&A*, **542**, A49
 Brott I., et al., 2011, *A&A*, **530**, A115
 Cioni M.-R. L., et al., 2011, *A&A*, **527**, A116
 Crowther P. A., Schnurr O., Hirschi R., Yusof N., Parker R. J., Goodwin S. P., Kassim H. A., 2010, *MNRAS*, **408**, 731
 Crowther P. A., et al., 2016, *MNRAS*, **458**, 624
 Drew J. E., Herrero A., Mohr-Smith M., Monguió M., Wright N. J., Kupfer T., Napiwotzki R., 2018, *MNRAS*,
 Evans C. J., et al., 2010, *ApJ*, **715**, L74
 Evans C. J., et al., 2011, *A&A*, **530**, A108
 Fujii M. S., Portegies Zwart S., 2011, *Science*, **334**, 1380
 Gaia Collaboration et al., 2016, *A&A*, **595**, A1
 Gaia Collaboration Brown A. G. A., Vallenari A., Prusti T., de Bruijne J. H. J., Babusiaux C., Bailer-Jones C. A. L., 2018, ArXiv:1804.09365,
 Gruendl R. A., Chu Y.-H., 2009, *ApJS*, **184**, 172
 Gvaramadze V. V., Weidner C., Kroupa P., Pfamm-Altenburg J., 2012, *MNRAS*, **424**, 3037
 Hénault-Brunet V., et al., 2012, *A&A*, **545**, L1
 Köhler K., et al., 2015, *A&A*, **573**, A71
 Kuiper R., Yorke H. W., Turner N. J., 2015, *ApJ*, **800**, 86
 Lada C. J., Lada E. A., 2003, *ARA&A*, **41**, 57
 Lamb J. B., Oey M. S., Segura-Cox D. M., Graus A. S., Kiminki D. C., Golden-Marx J. B., Parker J. W., 2016, *ApJ*, **817**, 113
 Langer N., Norman C. A., de Koter A., Vink J. S., Cantiello M., Yoon S.-C., 2007, *A&A*, **475**, L19
 Lennon D. J., et al., 2018, ArXiv:1805.08277,
 Luks T., Rohlfs K., 1992, *A&A*, **263**, 41
 Meixner M., et al., 2006, *AJ*, **132**, 2268
 Oh S., Kroupa P., 2016, *A&A*, **590**, A107
 Parker R. J., Goodwin S. P., 2007, *MNRAS*, **380**, 1271
 Pietrzyński G., et al., 2013, *Nature*, **495**, 76
 Platais I., van der Marel R. P., Lennon D. J., Anderson J., Bellini A., Sabbi E., Sana H., Bedin L. R., 2015, *AJ*, **150**, 89
 Platais I., et al., 2018, *AJ*, **156**, 98
 Poveda A., Ruiz J., Allen C., 1967, *Boletín de los Observatorios Tonantzintla y Tacubaya*, **4**, 86
 Rakavy G., Shaviv G., 1967, *ApJ*, **148**, 803
 Renzo M., et al., 2018, ArXiv:1804.09164,
 Rosen A. L., Krumholz M. R., McKee C. F., Klein R. I., 2016, *MNRAS*, **463**, 2553
 Rubio-Díez M. M., Najarro F., García M., Sundqvist J. O., 2017, in Eldridge J. J., Bray J. C., McClelland L. A. S., Xiao L., eds, IAU Symposium Vol. 329, The Lives and Death-Throes of Massive Stars. pp 131–135, doi:10.1017/S1743921317002447
 Sabbi E., et al., 2012, *ApJ*, **754**, L37
 Schneider F. R. N., Langer N., de Koter A., Brott I., Izzard R. G., Lau H. H. B., 2014, *A&A*, **570**, A66
 Schneider F. R. N., Castro N., Fossati L., Langer N., de Koter A., 2017, *A&A*, **598**, A60
 Schneider F. R. N., et al., 2018, *Science*, **359**, 69
 Townsley L. K., Broos P. S., Feigelson E. D., Garmire G. P., Getman K. V., 2006, *AJ*, **131**, 2164
 Townsley L. K., Broos P. S., Garmire G. P., Bouwman J., Povich M. S., Feigelson E. D., Getman K. V., Kuhn M. A., 2014, *ApJS*, **213**, 1
 Udalski A., et al., 2008, *Acta Astron.*, **58**, 329
 Walborn N. R., Barbá R. H., Sewilo M. M., 2013, *AJ*, **145**, 98
 Ward J. L., Kruijssen J. M. D., 2018, *MNRAS*, **475**, 5659
 Zapartas E., et al., 2017, *A&A*, **601**, A29
 Zinnecker H., Yorke H. W., 2007, *ARA&A*, **45**, 481
 de Koter A., Heap S. R., Hubeny I., 1997, *ApJ*, **477**, 792

AFFILIATIONS

- ¹ Astronomical Institute Anton Pannekoek, University of Amsterdam, 1098 XH Amsterdam, The Netherlands ² ESA, European Space Astronomy Centre, Apdo. de Correos 78, E-28691 Villanueva de la Cañada, Madrid, Spain ³ Department of Physics & Astronomy, Johns Hopkins University, Baltimore, MD 21218, USA ⁴ Space Telescope Science Institute, 3700 San Martin Drive, Baltimore, MD 21218, USA ⁵ Department of Physics and Astronomy, Hicks Building, Hounsfield Road, University of Sheffield, Sheffield S3 7RH, UK ⁶ UK Astronomy Technology Centre, Royal Observatory Edinburgh, Blackford Hill, Edinburgh, EH9 3HJ, UK ⁷ National Research Council, Herzberg Astronomy & Astrophysics, 5071 West Saanich Road, Victoria, BC, V9E 2ET, Canada ⁸ School of Astronomy & Space Science, University of the Chinese Academy of Sciences, Beijing 100012, China ⁹ National Astronomical Observatories, Chinese Academy of Sciences, Beijing 100012, China ¹⁰ Argelander-Institut für Astronomie, Universität Bonn, Auf dem Hügel 71, 53121, Bonn, Germany ¹¹ Centro de Astrobiología, CSIC-INTA, Carretera de Torrejón a Ajalvir km-4, E-28850 Torrejón de Ardoz, Madrid, Spain ¹² Institute of Astronomy, KU Leuven, Celestijnenlaan 200 D, B-3001 Leuven, Belgium ¹³ Department of Physics, University of Oxford, Keble Road, Oxford OX13RH, UK ¹⁴ Armagh Observatory, College Hill, Armagh BT619DG, UK

We thank P. Crowther, J. Heyl, M. C. Ramirez-Tannus, S. N. Shore, and S. Torres, and the HSTPROMO Collaboration for help and discussions. SdM acknowledges the European Unions Horizon 2020 research and innovation programme from the European Research Council (ERC), Grant agreement No. 715063 and VHB the NRC-Canada Plaskett Fellowship. This work has made use of data from the European Space Agency (ESA) mission *Gaia* (<https://www.cosmos.esa.int/gaia>), processed by the *Gaia* Data Processing and Analysis Consortium (DPAC, <https://www.cosmos.esa.int/web/gaia/dpac/consortium>).